



**MIDDLE EAST TECHNICAL UNIVERSITY
DEPARTMENT OF ELECTRICAL & ELECTRONICS
ENGINEERING**

**EE 464 - Static Power Conversion II - Term Project
Social Isolation Inc.**

Development of a DC-DC Converter for Battery Charging

Berkay UZUN - 2263812

Ali BELLİ - 2231421

Ahmet Halis SABIRLI – 2305225

TABLE OF CONTENTS

1. Project Definition	3
2. Topology Selection	3
3. Controller Selection	4
4. Transformer Design.....	6
4.1. Magnetic Core Selection	6
4.2. Winding Selection	11
4.3. Finite Element Analysis.....	12
5. Component Selection	15
5.1 Output Capacitor Selection	15
5.2 Controller Passive Elements Selection.....	16
5.2.1 Snubber Resistance and Capacitor Selection.....	16
5.2.2 Feedback Resistances Selection.....	17
5.2.3 $R_{I\text{REG}/SS}$ Selection.....	17
5.2.4 Sense Resistor Selection.....	18
5.2.5 Boundary Mode Detection Capacitor	18
5.2.6 Additional Component	19
5.3 Semiconductor Selection	19
5.3.1 Snubber Diodes Selection	19
5.3.2 MOSFET Selection.....	20
5.3.3 Output Diode Selection.....	21
6. LTspice Simulation Results	22
6.1 Steady-State Full-Load Responses.....	23
6.2 Load Regulation.....	25
6.3 Line Regulation	26
7. Cost analysis.....	27
8. Conclusion	28
9. References.....	29

1.PROJECT DEFINITION

In electrical cars, inside the vehicle, there are two different electrical systems which are low voltage and high voltage. The use of low voltage is to run the low power and low voltage components of the vehicle such as monitor, audio player or fans of the cooling system. To be able to charge the low voltage battery, there is a need of DC/DC converter between high voltage and low voltage system. The main motivation of the project is to construct an isolated 100W DC/DC converter which steps down the 220-400 V input to the 12 V output.

2. TOPOLOGY SELECTION

For the topology selection, there is only one main consideration which is the output power level. The selected topology must satisfy the output power and should not be over designed on it. To do that, we have made some research and found the source to decide the topology. From the information given in Table 1, there are 5 options [1].

Table 1 Power ranges of some of isolated DC-DC converter topologies

TOPOLOGY	POWER RANGE HISTORICALLY USED
Flyback	<100 W
Forward	50W-200W
Active Clamp Forward	50W-300W
Push-Pull	100W-500W
Half-Bridge	100W-500W
Full-Bridge	>500W

When we look at the options, the Full-Bridge is not suitable. In addition, we can see that Push-Pull and Half-Bridge may be over design for our application because the lower limit of them is satisfying the maximum power requirement of our system. Therefore, they are not suitable for our application. After that point, there are staying 3 different topologies. Forward and Active Clamp Forward has more component

compared to the Flyback converter and the Flyback converters maximum power limitation is satisfying our power level. Because of these reasons, we decided to use the Flyback topology to design the DC-DC converter. In addition to them, Flyback is a widely used topology and there are a lot of sources and controllers for this topology in power electronics field. Therefore, easy implementation of the topology has also made us to choose this topology.

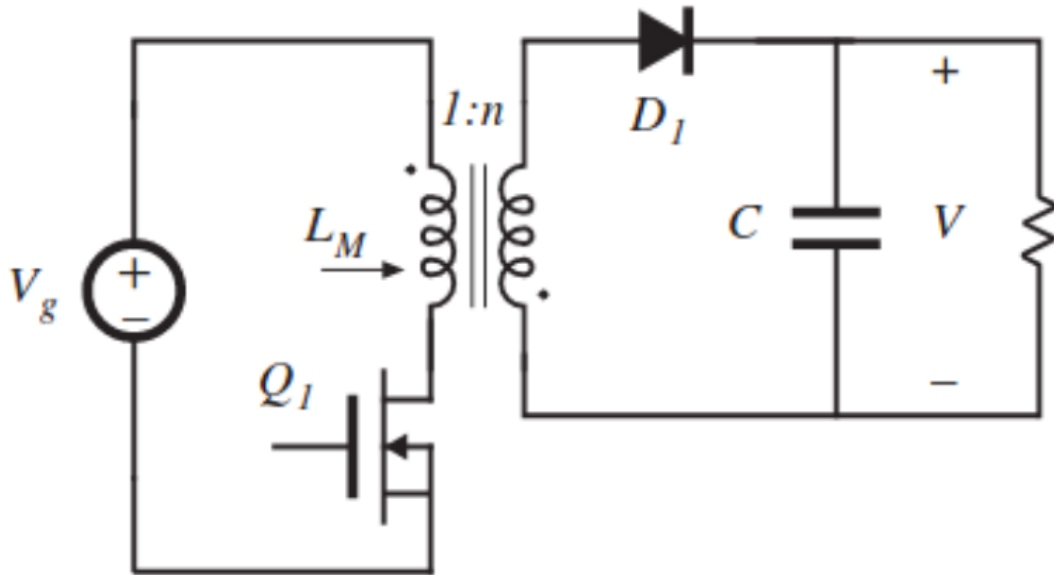


Figure 1 Flyback converter topology

3. CONTROLLER SELECTION

For the controller selection, we have only found two different controllers of the Analog Devices for our application. One of them is Forward and the other one is Flyback converter. The main limitation on the controllers is the maximum input voltage. Although, we have checked so many different producers' controllers, we did not find suitable controllers other than the LT8316 and LT3752-1. The main typical applications of the controllers are given in Fig.-1 and Fig.-2.

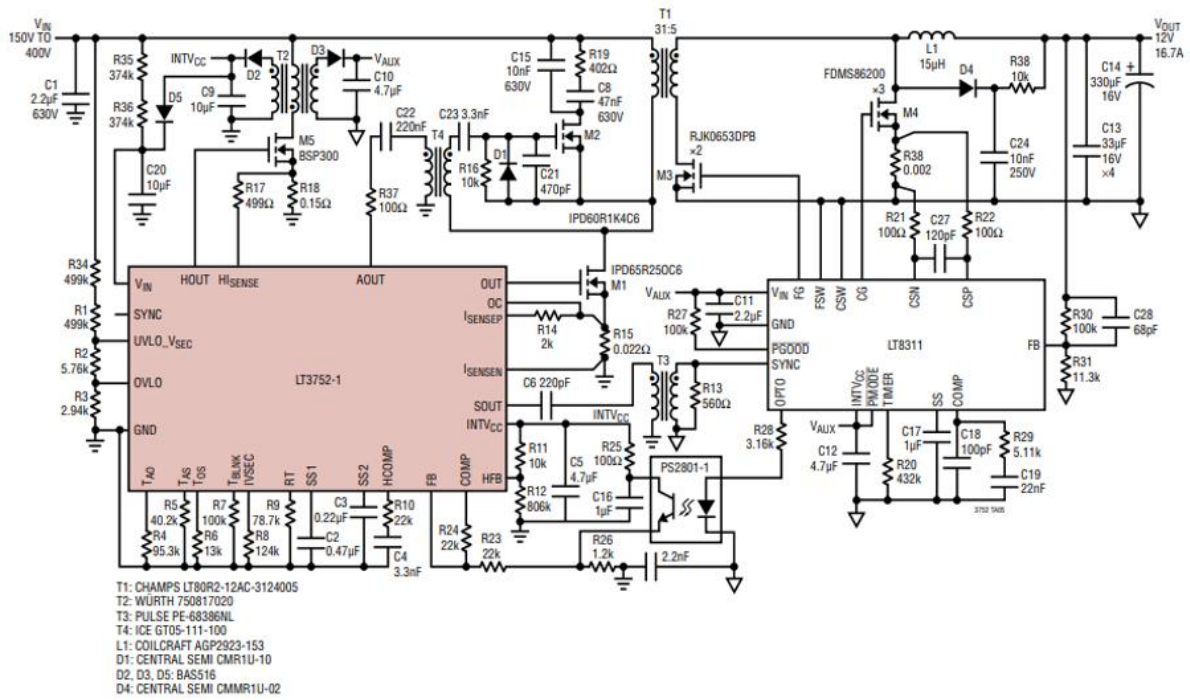


Figure 2 LT3752-1 Typical use

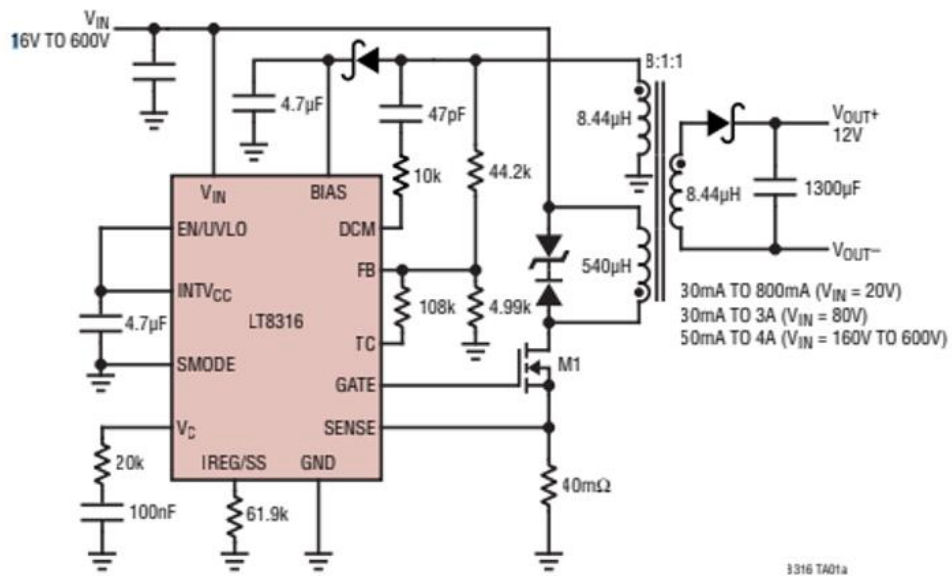


Figure 3 LT8316 Typical use

As the consideration given in the topology selection session, the Forward controller requires more component than the Flyback controller. Therefore, we have chosen the **LT8316 DC-DC Flyback controller** to develop the converter.

4. TRANSFORMER DESIGN

In this part of the project, the following steps were done, the Magnetic Core Design, Winding Selection and Finite Element analysis. To do that, at first, we examined the Flyback topology and developed an Excel program to find the proper interval of inductance and turning ratios. There are mainly two considerations to find the intervals, which are the properties of the controller and the requirements of the Flyback topology. Before going into the calculations of the controller, we calculated the topology requirements for these conditions. After that we obtained the controller needs and intervals. By considering the results, we decided on which core we will use. When we finished the core selection, we began to clarify the wiring properties which are depended on the effective window area of the core and current flowing through wirings. After completing the wire and core selection parts, we run a finite element on ANSYS to check whether our transformer going into the saturation or not. By proving the non-saturated behavior of the core during the maximum limits of the operation, we finished the Transformer Design part.

4.1. Magnetic Core Selection

Before going through the design, at first, we need to decide how we make design, in other words we need to fix some of the parameters to find the rest of the values. We decided to fix the desired duty cycle, desired current ripple, estimated efficiency, and the switching frequency. The switching frequency and the desired current ripple are fixed by considering the operation of the converter. After the fixing the values, the theoretical calculation of the Flyback topology going through like that,

$$\% \Delta I_L = 100 \text{ (For boundary discontinuous operation, nature of the controller)}$$

$$D_{max} = 0.35, f = 140 \text{ kHz}, \eta = 0.8$$

We need to find some important variables of the circuit to continue the calculations.

$$I_{out} = \frac{W_{out}}{V_{out}} = \frac{100}{12} = 8.34 \text{ A}$$

$$I_{out,average} = \frac{I_{out}}{1 - D} = \frac{8.34}{1 - 0.35} = 12.83 \text{ A}$$

$$N_{PS} = \frac{D}{1 - D} * \frac{V_{in,min}}{V_{out} + V_{diode}} = \frac{0.35}{1 - 0.35} * \frac{220}{12 + 0.5} = 9.47$$

The ratio is hard to find a proper turn numbers of the primary and secondary, therefore,

$$N_{PS} \approx 9$$

After deciding the turn, we need calculate estimated duty cycle of the system to find the turn number of the primary and secondary windings.

$$D_{estimated_max} = \frac{1}{1 + \frac{V_{in,min}}{V_{out}} * \frac{1}{N_{PS}}} = \frac{1}{1 + \frac{220}{12} * \frac{1}{9}} = 0.33$$

$$D_{estimated_min} = \frac{1}{1 + \frac{V_{in,max}}{V_{out}} * \frac{1}{N_{PS}}} = \frac{1}{1 + \frac{400}{12} * \frac{1}{9}} = 0.21$$

Now, let's find the maximum turn number of the primary side,

$$N_{P,max} = V_{out,max} * \frac{D_{estimated_min}}{f * A_c * B_{sat}}$$

As you can observe, we need the find a core to use the effective core area (A_c) and the saturation flux density (B_{sat}). Selecting the core is not straight forward issue. We selected it by checking the limitations again and again for different cores. The

limitations will be calculated later. We selected one of the cores of **TDK**, which is **ETD 29/16/10**. The selected core properties are given in the Table 2.

Table 2 Selected magnetic Mn-Zn ETD shape core

PROPERTIES	VALUES
Saturation Flux Density(T)	~0.39
Effective magnetic cross section(mm ²)	76
Window Area (Winding Cross Section) (mm ²)	97
Inductance Factor(nH/turn ²)	383
Average Length of Turn(mm)	52.8
Effective magnetic path length (mm)	70.4
Relative permeability of core material (Ungapped)	1470
Relative permeability of core material (Gapped)	281
Airgap(mm)	0.2

$$N_{P,min} = V_{out,max} * \frac{D_{estimated_min}}{f * A_c * B_{sat}} = \frac{400 * 0.213}{140 * 76 * 0.39 * 10^{-3}} = 20.53$$

$$N_{S,min} = \frac{N_{p,min}}{N_{PS}} = \frac{21.92}{9} = 2.28$$

We decided to use the primary turn as 25 and secondary as 3. Now, we need to calculate the final, effective, duty cycle,

$$D_{effective_max} = \frac{1}{1 + \frac{V_{in,min}}{V_{out}} * \frac{N_s}{N_p}} = \frac{1}{1 + \frac{220}{12} * \frac{3}{25}} = 0.31$$

Now, let's find the effective inductance values for %100 inductor current ripple,

$$L_{effect,sec} = \frac{V_{out} + V_{diode}}{1} * \frac{1 - D_{effective,max}}{f * I_{out,average}} * \frac{1}{\frac{\Delta I_L}{I_L}} = \frac{12.5 * 0.69}{140 * 12.83 * 10^3} * \frac{1}{1} = 4.8 \mu H$$

$$L_{effect,prim} = L_{effect,sec} * N_{PS}^2 = 333 \mu H$$

After finishing the theoretical calculations, now we need to find the limitations of the controller. There are 3 different minimum primary inductance limitation and one maximum primary inductance limitation. Before starting to the calculations, there are some parameters must be given which are used in the following calculations coming from the nature of the controller.

$$t_{off(min)} = 800 \text{ ns}$$

$$I_{SW(min)} = 20 \frac{mV}{R_{SNS}}, R_{SNS} \approx 28 \text{ m}\Omega$$

$$t_{on(min)} = 300 \text{ ns}$$

$$I_{SW(max)} = 100 \frac{mV}{R_{SNS}}$$

$$t_{BU} = 50 \text{ }\mu\text{s}$$

$$L_{min1} = t_{off(min)} * N_{PS} * \frac{V_{out} + V_{diode}}{I_{SW(min)}} = \frac{800 * 8.34 * 12.5 * 10^{-9}}{\frac{20}{28}} = 116 \text{ }\mu\text{H}$$

$$L_{min2} = t_{on(min)} * \frac{V_{in,max}}{I_{SW(min)}} = \frac{300 * 400 * 10^{-9}}{\frac{20}{28}} = 168 \text{ }\mu\text{H}$$

$$L_{min3} = 2 * (V_{out} + V_{diode}) * \frac{I_{out}}{\eta * I_{SW(max)}^2 * f} = \frac{2 * 12.5 * 8.34}{0.8 * \left(\frac{100}{28}\right)^2 * 140 * 10^3} = 146 \text{ }\mu\text{H}$$

$$L_{max} = \frac{0.8 * (V_{out} + V_{diode}) * (N_{PS} * t_{BU})}{I_{SW(max)}} = \frac{0.8 * 12.5 * 8.34 * 50 * 10^{-6}}{\frac{100}{28}} = 116.7 \text{ }\mu\text{H}$$

By using the core properties, we can calculate the primary and secondary inductances and check whether we stay in the controller specifications or not and whether we close to theoretical calculations.

$$L_{prim} = A_L * N_p^2 = 383 * 25^2 * 10^{-9} = 240 \text{ } \mu H$$

$$L_{sec} = A_L * N_s^2 = 383 * 3^2 * 10^{-9} = 3.47 \text{ } \mu H$$

The selection of the inductance factor (A_L) is not a straightforward issue and we selected it by considering the saturation limit of the selected core. Therefore, we have had to lose some inductance to satisfy the non-saturated operation and to leave the final duty cycle lower than the desired one. As a result, the inductance values are suitable for the controller and the controller will handle rest of the parameters by using the feedback loop inside it.

We checked how much airgap we need to stay in the non-saturated region during the operation,

$$Gap_{min} = \mu_o * N_p^2 * \frac{A_e}{L_{primary}} - \frac{l_e}{\mu_e} = 4 * \pi * 10^{-7} * 25^2 * \frac{76 * 10^{-6}}{240 * 10^{-6}} - \frac{70.4 * 10^{-3}}{1470}$$

$$Gap_{min} = 0.2 \text{ mm}$$

We have used the equation given below to check whether the core is going through the saturation during the operation or not,

$$B_{max} = \mu_o * \mu_e * N_p * \frac{I_{in,max}}{I_e} = \frac{4 * \pi * 10^{-7} * 281 * 25 * \left(\frac{100}{220 * (0.31)} * 2 \right)}{70.4 * 10^{-3}}$$

$$B_{max} = 0.37 \text{ T} < 0.39 \text{ T}$$

We are satisfying saturation condition, which is the most important one for the application. At that point, we are finishing the core selection part and moving to the winding selection part.

4.2. Winding Selection

Winding selection is another important topic while designing a transformer. Both the wire itself and the wiring type effects the performance of the transformer. Choosing thicker wire may seem to reduce the resistance and losses however due to skin and proximity effects, diameter of the wire does not affect losses after a point. Moreover, thicker wires result in bulkier windings which increases leakage inductances. However, choosing wires too thin may result in excessive heat generation and meltdown in critical points of the winding. Therefore, we tried to make a balanced selection.

First, we assumed that output current flows through the windings without alternating and find a wire so that current density of the wire is around 5 A/mm²

$$I_{out} = 8.34 \text{ A}$$

$$A_{wire} = \frac{I}{J} = \frac{8.34}{5} = 1.668 \text{ mm}^2$$

$$D_{wire} = 1.458 \text{ mm}$$

Even though, due to skin and proximity effects, current will flow nonhomogeneous and most of the copper will not carry any current, high heat capacitance of thicker wire will prevent burnouts in the winding.

We have total of 31 turns of winding which consists of 25 primary, 3 secondary and 3 feedback turns. The selected core can accommodate around 12-13 turns per layer. Since we only needed three layers of windings, we did not see necessary to make interleaved winding and make two layers of primary winding and one layer of combined secondary and feedback winding. In this case, we chose **AWG15 cable**.

4.3. Finite Element Analysis

After deciding the core material, shape, airgap and the windings, we started to draw the transformer in Maxwell 3D. For faster analysis, continuous surfaces were drawn with edges as shown in Fig 5. Main reason of Finite Element Analysis is to check our design parameters and calculate transformer parameters which cannot be calculated analytically. First, we draw only the primary winding to check our model's validity. After finding that analysis results were almost same with datasheet values of the core we continued with secondary and feedback windings. However, if we make 25 turn primary and 3 turn secondary, secondary inductance becomes larger than the calculations. This is most probably due to reduction of magnetic path (therefore reduction in reluctance) while increasing layer number (winding radius). This kind of secondary effects was the first reason why we did finite element analysis. To overcome this effect, we reduced the secondary turn number to 2.5 and the results were satisfactory.

	Current1	Current3	Current5
Current1	244.11	28.622	28.607
Current3	28.622	3.5545	3.3315
Current5	28.607	3.3315	3.5369

Figure 4. Self and mutual inductances of the windings (μH)

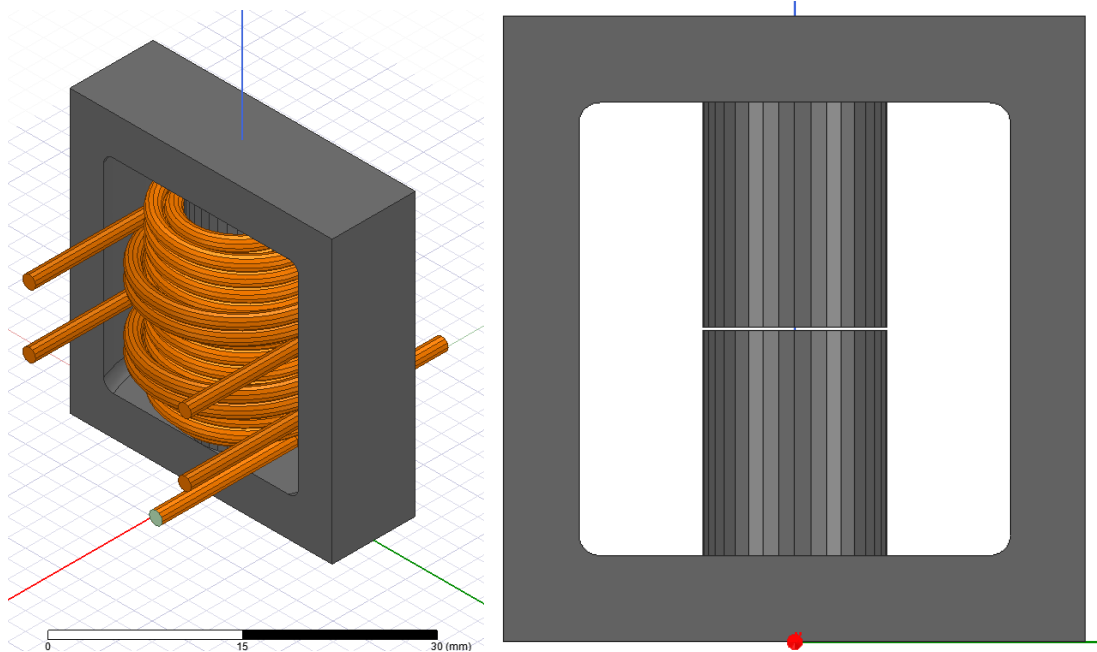


Figure 5 Maxwell 3D model

After satisfying inductance and turn ratio parameters we moved on to saturation control. To observe the magnetic flux density in most extreme case, we supplied primary winding with 3A current. This 3A comes from the calculations of the controller and it is also observed in LTspice. To ease the work of the computer, meshing was concentrated in the inner corner and near the airgap. Both magnetic flux density and vectors can be seen in Fig 6,7 and 8.

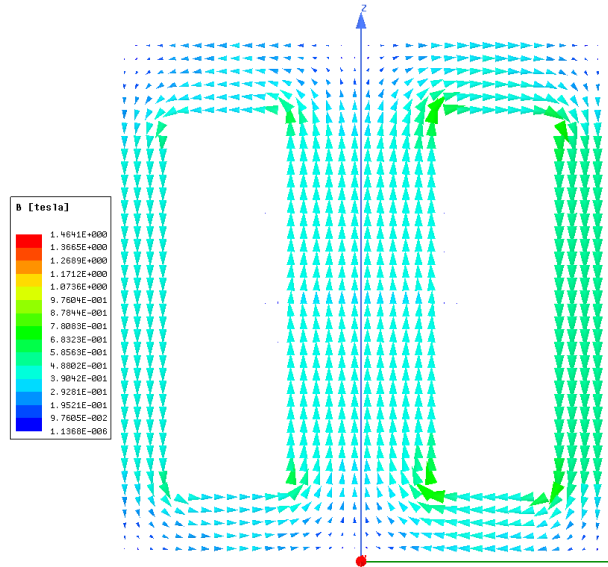


Figure 6 Magnetic flux vectors

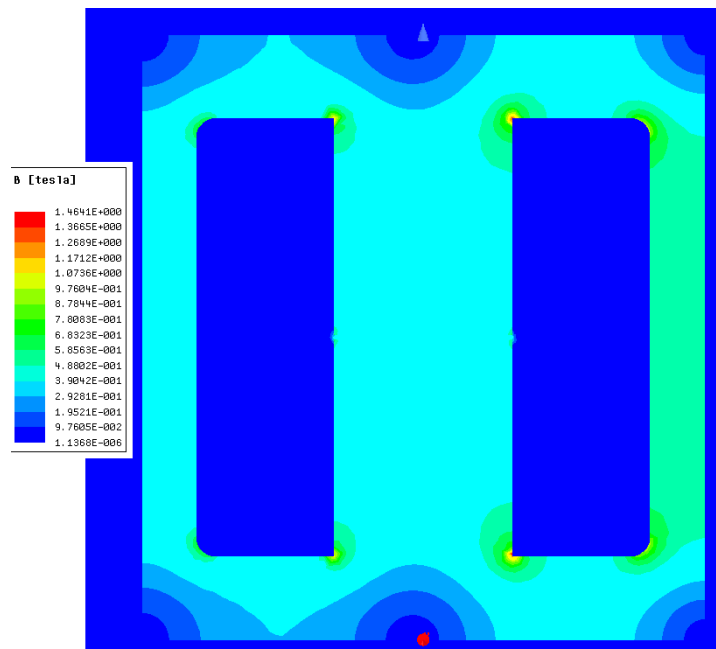


Figure 7 Magnetic flux density

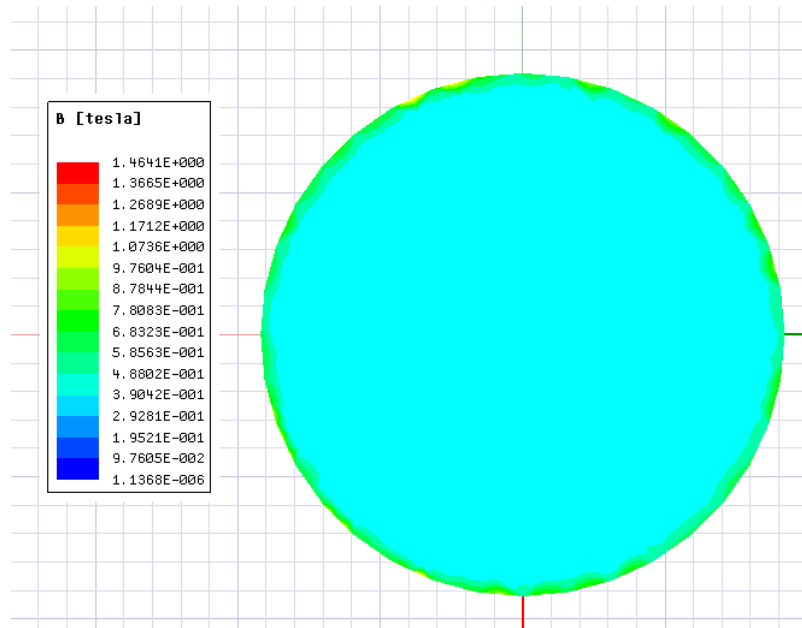


Figure 8 Magnetic flux density of the core center

At maximum magnetic flux density that the core can see, most of the core remains unsaturated. However, some corners of the core are saturated. This may be acceptable since transformer will work in this condition on extreme cases and for transient times. Transformer current will reduce after reaching steady state.

Final analysis that we made is eddy current analysis. We made this analysis to estimate the AC resistance of the windings and to observe the current density in those windings. Current density can be seen in Fig 9.

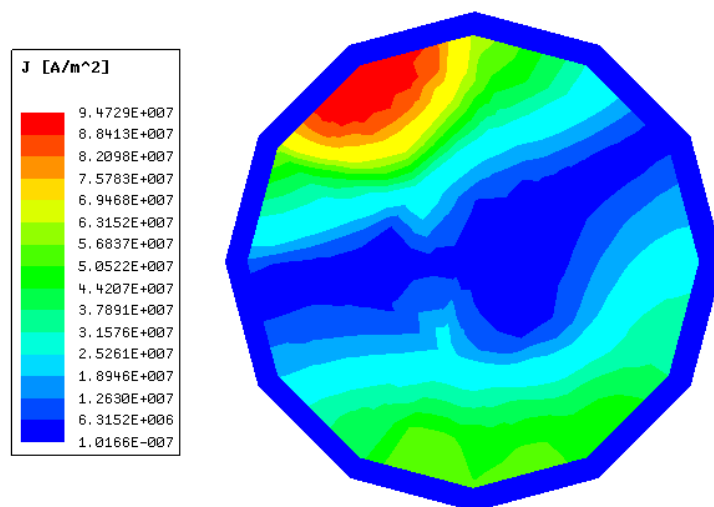


Figure 9 Current density of a single wire in primary winding

As expected, we see nonhomogeneous current distribution in the conductor due to skin and proximity effects. More important than to see the current distribution is to get the AC resistance to accurately calculate copper losses in the transformer.

Freq:	1e-012Hz	Freq:	140000Hz
	Current1		Current1
Current1	10.912	244.13	Current1
			1869.7
			235.66

Figure 10 DC and AC resistances of primary winding (mΩ)

As we can see in Fig 10. Frequency has a significant effect on the resistance. Even though we expected such increase, numerical value of the resistance is found by FEA. Therefore, we used this result (1.869Ω) in LTspice simulations.

5. COMPONENT SELECTION

For the component selection part, there are 3 main subtitles, which are the output capacitor selection, controller passive elements selection and the power semiconductor selection for now to complete the simulations. When we begin to develop the PCB schematics and layouts, there will be also connector selection part and elements of protection circuits.

5.1 Output Capacitor Selection

The output capacitor should be selected to reduce output voltage ripple while also keeping in view the larger size and price of a larger capacitor. The minimum output capacitor can be calculated using the equation as below:

$$C_{out,min} = \frac{L_{prim} * I_{lim}^2}{2 * V_{ripple} * V_{out}} = \frac{244.11 * 10^{-6} * \left(\frac{100 * 10^{-3}}{27.62 * 10^{-3}}\right)^2}{2 * 0.48 * 12} = 277.77 \mu F$$

where I_{lim} = Maximum primary current = 100mV/ R_{sense}

In this equation, we found the minimum output capacitor value that is required. However, we chose around 438 μF capacitor for better filtering. Also, we aimed to minimize ESR. For this reason, we choose following capacitors:

Type	Value	Quantity
Aluminum	100 μF	3
Ceramic	47 μF	2
Ceramic	10 μF	4
Ceramic	1 μF	4

5.2 Controller Passive Elements Selection

5.2.1 Snubber Resistance and Capacitor Selection

The proposed design solution for the RC snubber is to power up at low voltage to prevent overvoltage stress, calculate the duration of the ringing on the MOSFET's drain when the power switch turns off without the snubber, and then apply capacitance $C_{Snubber}$ until the ringing period is 1.5 to 2 times longer. To find the snubber resistance, we first need to find leakage inductance. The leakage inductance depends on the coupling coefficient. Coupling coefficients of $k=99$ percent are typical, and they are determined by the transformer's structure and materials.

$$L_{leak} = \frac{2 * L_{pri}(1 - k)}{k} = 2 * 244.11 * 10^{-6} * \frac{1 - 0.99}{0.99} = 4.93 \mu H$$

Now, we can find the snubber resistance with equation below. The capacitor value here is taken from the datasheet of the mosfet we have chose.

$$R_{Snubber} = \sqrt{\frac{L_{leak}}{C_{in}}} = \sqrt{\frac{4.93 * 10^{-6}}{1150 * 10^{-12}}} = 65.47 \Omega$$

Component	Type	Value
Snubber Resistance	Chip Resistor-Surface Mount	68Ω
Snubber Capacitor	Ceramic	470pF

5.2.2 Feedback Resistances Selection

The isolated output voltage is controlled by the LT8316 using a special sampling scheme. The scheme experiences repeatable delays and error sources due to its sampling design, which would influence the output voltage and cause a reevaluation of the resistor values. So, the controller needs feedback resistors to regulate this situation. According to the datasheet, in order to determine the values of these resistors, we need to assign a value to one of them and find the other with the equation below.

$$R_{fb1} = 10 \text{ k}\Omega \text{ (fixed value)}$$

$$R_{fb2} = R_{fb1} * \left(\frac{V_{out} + V_{diode}}{1.22} * N_{TS} - 1 \right) = 10 * 10^3 * \left(\frac{12 + 0.5}{1.22} * 1 - 1 \right) = 92.45 \text{ k}\Omega$$

Resistance	Type	Value
R _{fb1}	Chip Resistor-Surface Mount	10kΩ
R _{fb2}	Chip Resistor-Surface Mount	90kΩ

5.2.3 R_{I_{REG/SS}} Selection

This resistor is used to regulate the output current. We can find the resistance value we need to use with the equation given below:

$$R_{I_{REG/SS}} = \frac{2.5M\Omega * I_{out} * R_{sense}}{N_{PS}} = \frac{2.5 * 10^6 * \frac{100}{12} * 27.62 * 10^{-3}}{8.34} = 68.9 \text{ k}\Omega$$

According to the above equation, we found the required resistance value of 68.9kΩ.

Type	Value
Chip Resistor-Surface Mount	69.8kΩ

5.2.4 Sense Resistor Selection

We need a sense resistor to be able to set the maximum current. In the datasheet of the controller we chose, the formula for R_{sense} is shown as below:

$$R_{sense} = \frac{1 - D_{V_{in}(min)}}{I_{out(max)}} * 50mV * N_{ps} * 0.8 = \frac{1 - 0.31}{\frac{100}{12} * 2} * 50 * 10^{-3} * 8.34 * 0.8$$

$$R_{sense} = 27.62 m\Omega$$

Type	Value
Chip Resistor-Surface Mount	28mΩ

5.2.5 Boundary Mode Detection Capacitor

Application note of the controller suggest using 47pF capacitor and check if the operating point is in boundary condition. If not, it is suggested to increase this capacitor up to 100pF. 47pF was satisfactory for our application so we selected this value.

Type	Value
Ceramic	47pF

5.2.6 Additional Component

C_{DRV} , C_{BIAS} and V_c capacitor, V_c resistance, DCM resistance, thermal correction resistance and are not specified as application dependent capacitors in the datasheet. Therefore, we used same values capacitors as given in the typical application.

Bias diode is also not specified in the application note but it is denoted with fast diode symbol. We will choose this diode according to the simulation results.

Component	Type	Value
V_c Resistance	Chip Resistor-Surface Mount	20k Ω
Thermal Correction Resistance	Chip Resistor-Surface Mount	500k Ω
DCM Resistance	Chip Resistor-Surface Mount	10k Ω
Bias Capacitor	Ceramic	4.7 μ F
Drive Capacitor	Ceramic	4.7 μ F
V_c Capacitor	Ceramic	100nF

Type	Package	Maximum Voltage (V)	Maximum Current (A)
Schottky	DO-214AC	150	3A

5.3 Semiconductor Selection

5.3.1 Snubber Diodes Selection

Fast recovery: According to the application note, breakdown voltage of this diode must be greater than the drain pin voltage of the MOSFET.

Type	Package	Maximum Voltage (V)	Maximum Current (A)
Fast Recovery	DO-214AC	600	2A

Zener: Zener voltage must be largest possible value withing given limitations. And it is recommended to use around 500 mV Zener diode in the snubber. According to the controller's datasheet, we can calculate the maximum voltage capacity of the Zener diode with the following equation:

$$V_{zener} \leq V_{breakdown} - V_{in,max}$$

$$V_{zener} \leq 650V - 400V$$

$$V_{zener} \leq 250V$$

Type	Package	Maximum Voltage (V)	Maximum Power (W)
Zener	SMB	150	3

5.3.2 MOSFET Selection

As can be seen from the simulation result in Figures 11 and 12, the maximum voltage is around 450V and current value is around 3.6A on the MOSFET. While choosing the MOSFET, we made a choice considering these values.

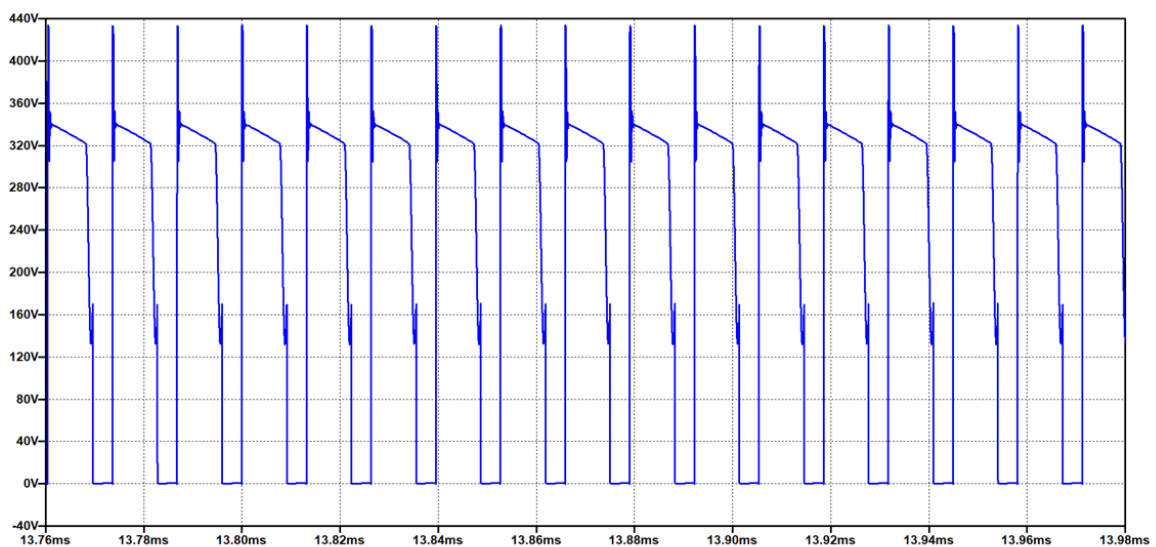


Figure 11 MOSFET voltage graph

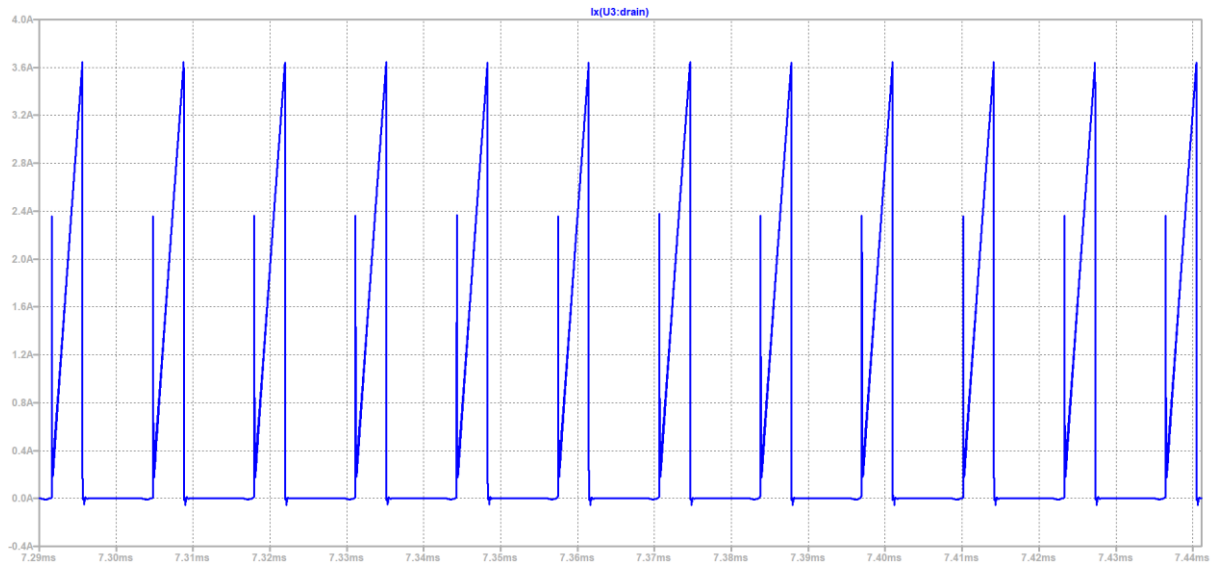


Figure 12 MOSFET current graph

Type	Package	Maximum Voltage (V)	Maximum Current (A)
CoolMOS™	PG-TO252-3	650	13A

5.3.3 Output Diode Selection

The Figures below, namely Figure 13 and Figure 14, show the reverse voltage of the diode and the peak forward current. According to these graphs, the reverse voltage on the diode is around 65V. The current flowing on it is approximately 35 A. We should choose the output diode by considering these criteria.

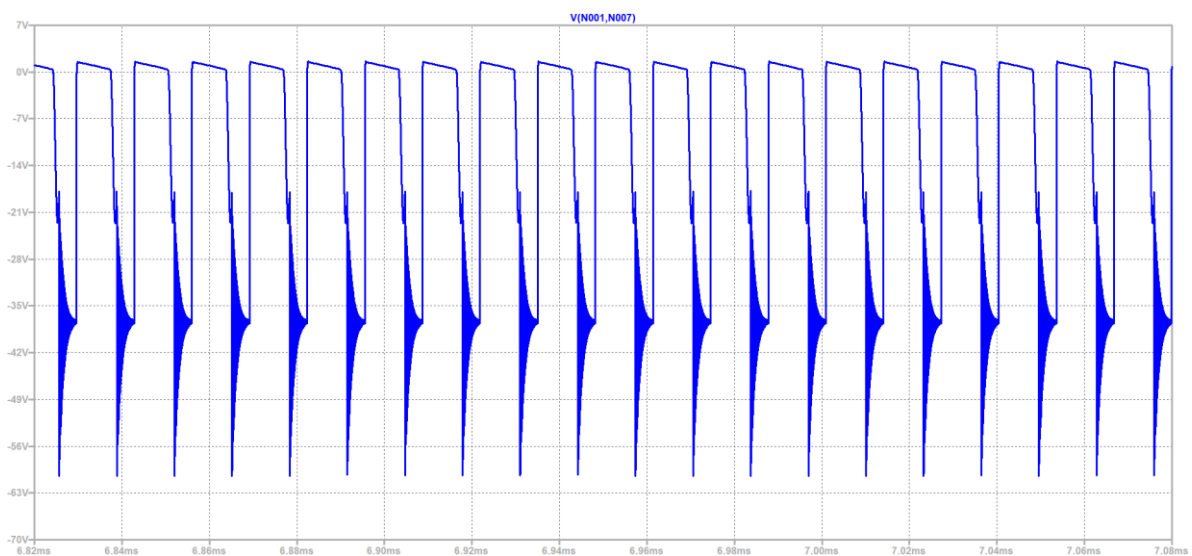


Figure 13 Output diode voltage graph

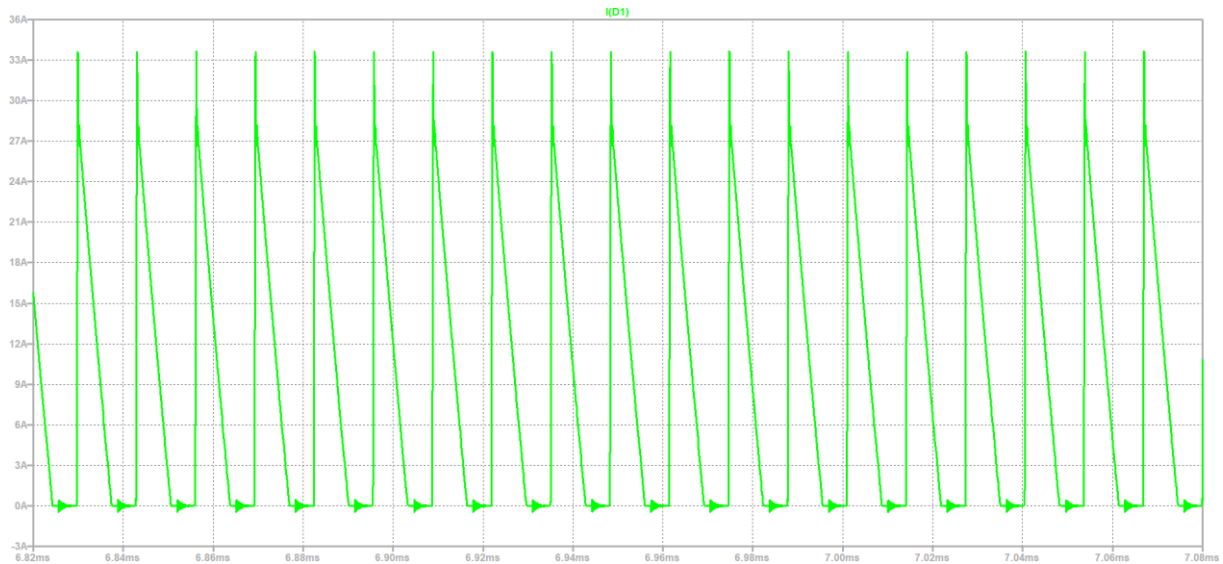


Figure 14 Output diode current graph

Type	Package	Maximum Voltage (V)	Maximum Current (A)
Schottky	TO-277	80	20

6. LTSPICE SIMULATION RESULTS

We divided LTspice simulation results into three subtitles, which are Steady-State Full-Load Responses, Load Regulation and Line Regulation. To do that, we constructed all the circuit on the LTspice by reducing the ideality of the circuit by adding some of the real-time application parameters such as Leakage inductances and series resistance of the primary and secondary side of the transformer. The overall simulation model is given in the Fig.15.

```
.lib C:\Users\Ali Belli\Documents\LTspiceXVII\lib\sub\sub\NEW.lib
```

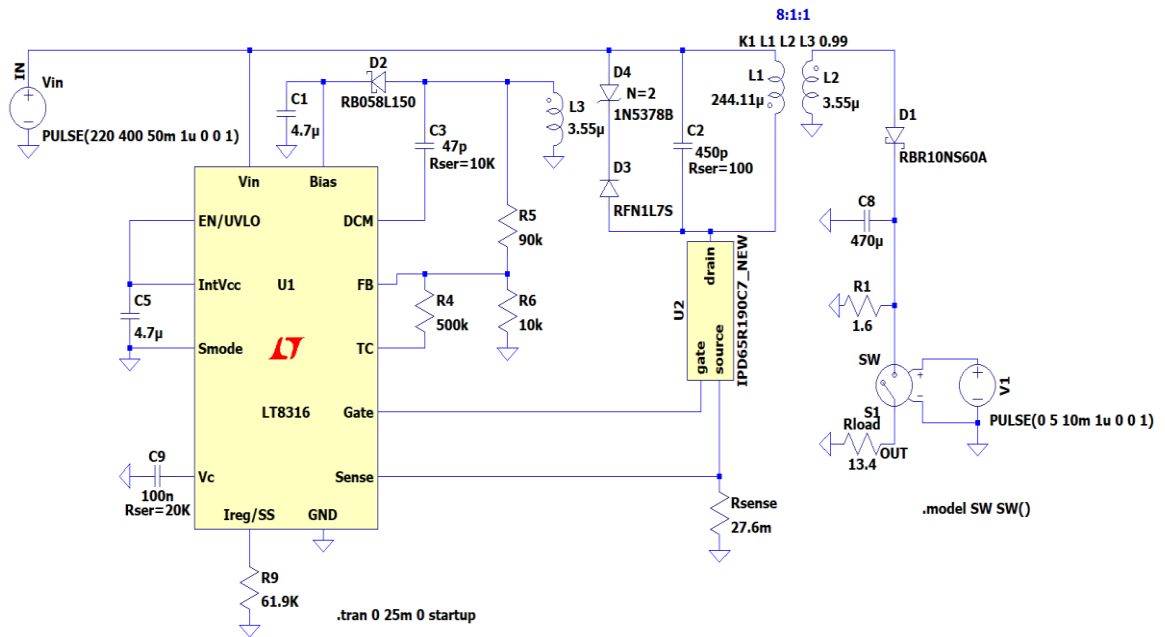


Figure 15 Project design schematic

6.1 Steady-State Full-Load Responses

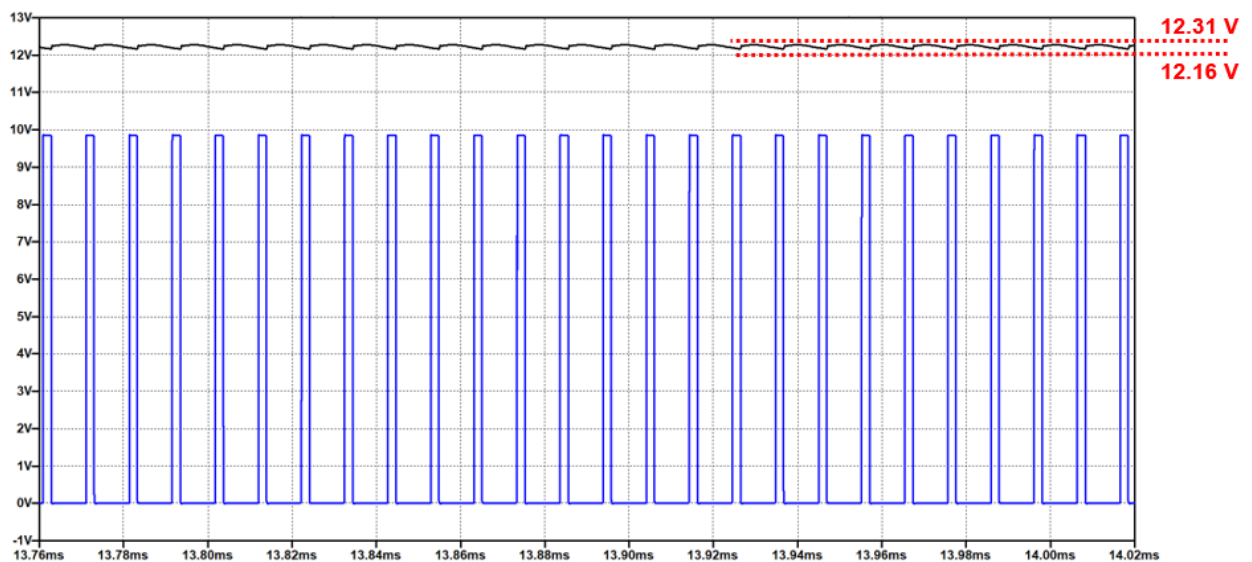


Figure 16 Output Voltage at 400 V input

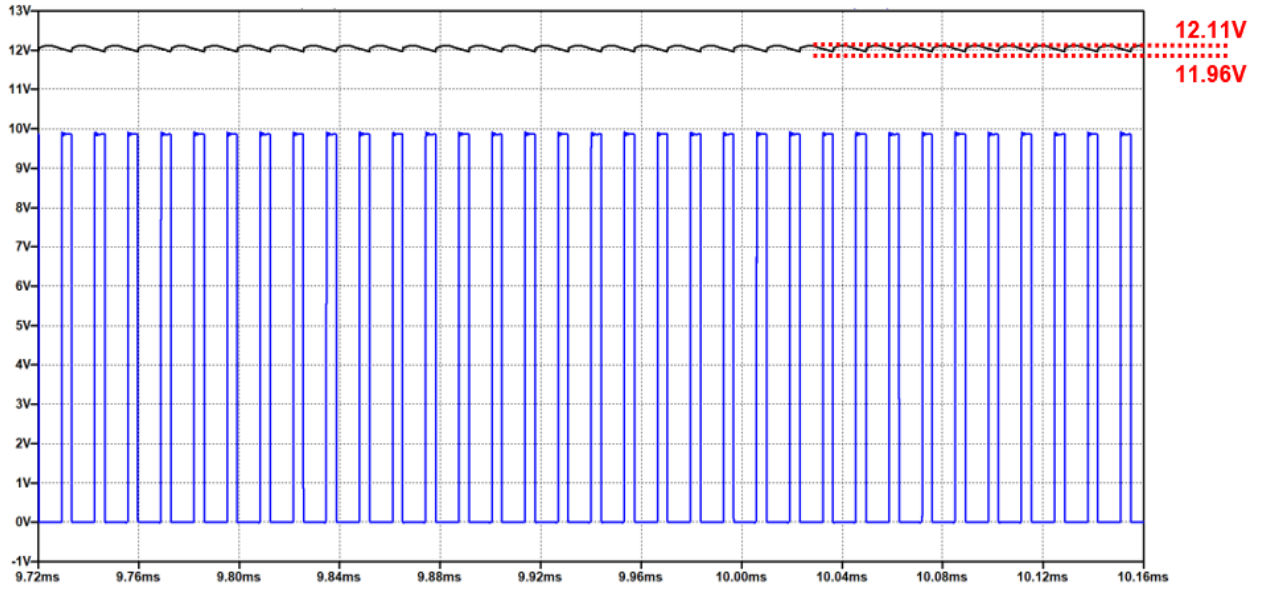


Figure 17 Output Voltage at 220 V input

From the steady-state full load analysis of the converter at 400 V maximum input and 220 V minimum input conditions, which are given in the Fig.16 and Fig. 17 respectively, we can claim that the output voltage of the controller is including ripple less than %4. As a proof,

$$\% \Delta V_{out,220} = \frac{12.11 - 11.96}{12} * 100 = \%1.25 < \%4$$

$$\% \Delta V_{out,400} = \frac{12.31 - 12.16}{12} * 100 = \%1.25 < \%4$$

6.2 Load Regulation

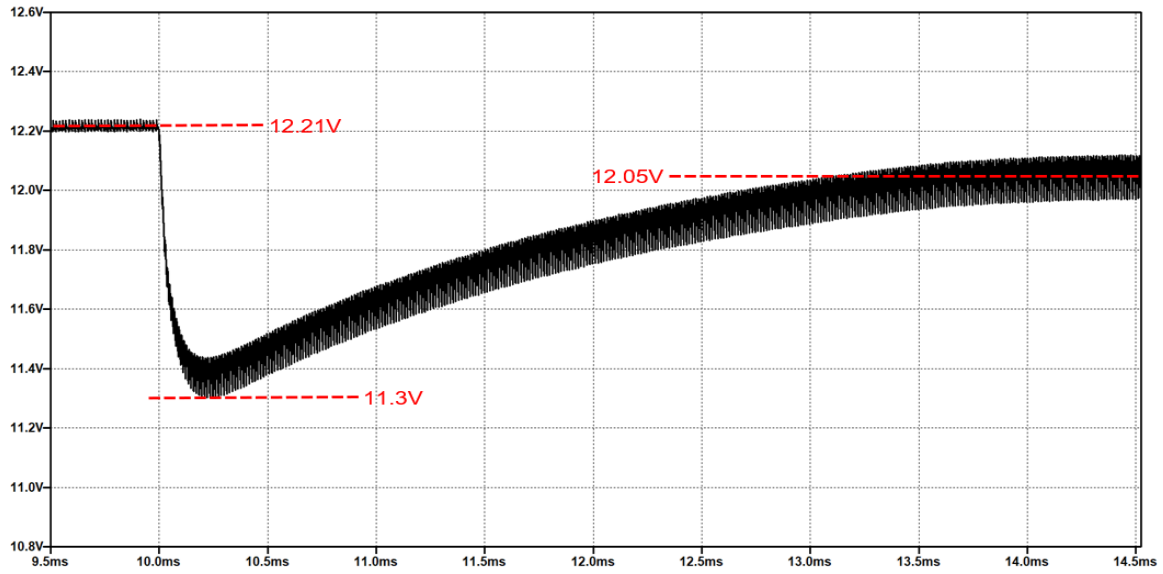


Figure 18 Light Load to Full Load Response

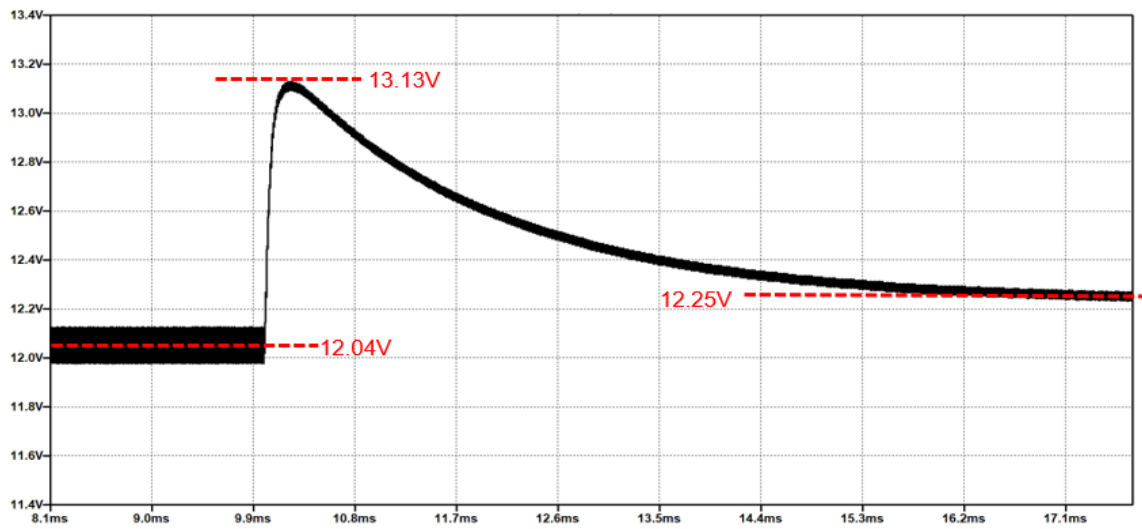


Figure 19 Full Load to Light Load Response

The load regulation simulations were conducted as two part, which are heavy load to light load and vice versa. The results are given in Fig. 18 and Fig. 19. From the figures, we can say that the results are satisfying the load regulation limitation. As a proof,

$$\% \Delta V_{out,load1} = \frac{12.21 - 12.05}{12} * 100 = \%1.33 < \%3$$

$$\% \Delta V_{out,load2} = \frac{12.25 - 12.04}{12} * 100 = \%1.75 < \%3$$

6.3 Line Regulation

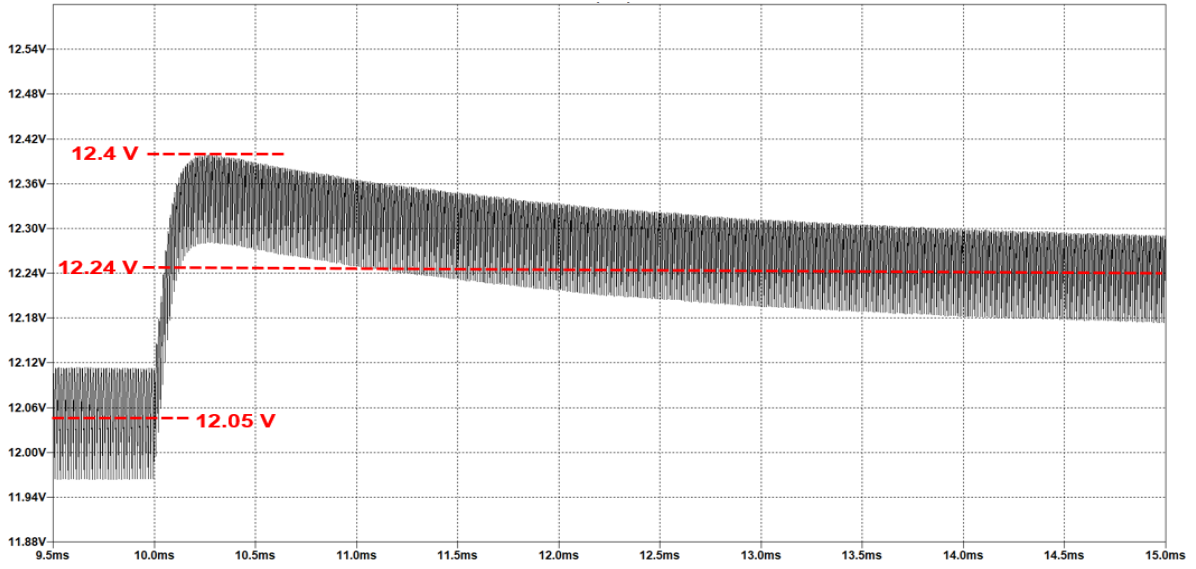


Figure 20 220V to 400V Response

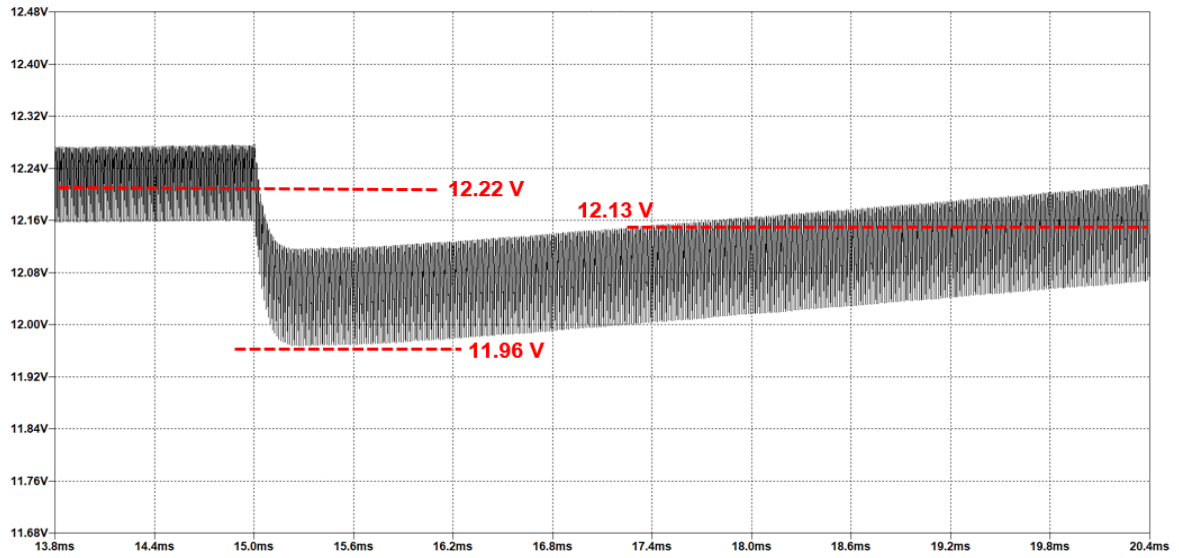


Figure 21 400V to 220V Response

The line regulation simulations were conducted as two part, which are 220 V input to 400V and vice versa. The results are given in Fig. 20 and Fig. 21. From the figures, we can say that the results are satisfying the line regulation limitation. As a proof,

$$\% \Delta V_{out,line1} = \frac{12.24 - 12.05}{12} * 100 = \%1.58 < \%3$$

$$\% \Delta V_{out,line2} = \frac{12.22 - 12.13}{12} * 100 = \%0.75 < \%3$$

7. COST ANALYSIS

The table below shows the cost analysis of the components we have selected.
The price of the components is calculated over 1000 pieces.

Table 3 Cost Analysis of the Design

Manufacturer	Digi-Key Part Number	Quantity	Unit Price (\$)	Price (\$)
Analog Devices Inc.	LT8316IFE#PBF-ND	1000	3.345	3345
Infineon Technologies	IPD65R190C7ATMA1CT-ND	1000	1.5764	1576.4
EPCOS - TDK Electronics	495-5450-ND	2000	0.3978	795.6
KEMET	399-EDH107M016A9GAATR-ND	3000	0.09439	283.17
Venkel	2679-C1206X5R160-476MNETR-ND	2000	0.68749	1374.98
Samsung Electro-Mechanics	1276-1096-2-ND	4000	0.01912	76.48
Taiyo Yuden	587-5514-1-ND	4000	0.01524	60.96
Venkel	2679-LCR2512-R028FTTR-ND	1000	0.18927	189.27
Yageo	311-69.8KCRCT-ND	1000	0.00759	7.59
Yageo	311-20.0KHRCT-ND	1000	0.00436	4.36
Samsung Electro-Mechanics	1276-3431-1-ND	2000	0.00695	13.9
Vishay Dale	BC4966CT-ND	1000	0.22296	222.96
Vishay Dale Thin Film	764-1550-2-ND	1000	0.22	220
TE Connectivity Passive Product	A121294CT-ND	1000	0.21173	211.73
Taiyo Yuden	587-4896-1-ND	1000	0.08622	86.22
TDK Corporation	445-7479-1-ND	1000	0.07245	72.45
Würth Electronic	732-7532-1-ND	1000	0.01548	15.48
AVX Corporation	478-1282-1-ND	1000	0.02875	28.75
Yageo	311-3383-1-ND	1000	0.03305	33.05
Rohm Semiconductor	RB058L150TE25TR-ND	1000	0.15068	150.68
Diodes Incorporated	1SMB5953B-13DI-ND	1000	0.13613	136.13
ON Semiconductor	SURA8260T3GOSCT-ND	1000	0.16027	160.27
Taiwan Semiconductor Corporation	TSPB20U80SS2G-ND	1000	0.6276	627.6
Remington Industries	2328-15SNSP.125-ND	250	9.48	2370
				12063.03

8. CONCLUSION

This report includes the topology selection, controller selection after topology selection, transformer design, component selection and overall simulation results of the converter parts.

For the simulation part of the project, there are some important parts of the project must be completed before going on details of simulation. At first, a topology must had been selected and we selected the Flyback topology. After topology selection, we found a controller which satisfies the needs of the system. In addition, there is a need for a transformer as we use Flyback topology. There is a need to develop a tool to decide on the properties of the transformer. An Excel program is developed to fix the features of the transformer. When we finished the transformer design part, we run a finite element analysis on the ANSYS to prove the non-saturated behavior of the converter during the operation. After that, we continued with the passive element selection of the converter and selection of the semiconductor devices of the flyback topology and snubber circuit. When the component selections and the transformer design parts are completely done, we conducted the simulations and prove that the converter satisfies the features wanted at the project definition.

The main purpose of the report is to prove that the designed converter is satisfying the musts, and at the end of it, we can claim that we are satisfying all needs of the project.

9. REFERENCES

1. Topology Key to Power Density in Isolated DC-DC Converters. (n.d.). Retrieved April 27, 2021, from <https://www.powerelectronics.com/technologies/dc-dc-converters/article/21854364/topology-key-to-power-density-in-isolated-dcdc-converters>